Robust Multi-Objective Control Design for Underground Coal Gasification Energy Conversion Process

ARTICLE HISTORY
Compiled March 1, 2018

ABSTRACT
The efficiency of an underground coal gasification (UCG) process can be increased if the heating value of the product gases is kept at the desired level for a longer period of time. In literature, this task has been accomplished by using model based control strategies, which employ the complex nonlinear models of the process. In order to exploit the flexibility of the linear control design methodologies, a linear model of the UCG process has been developed, which retains the dynamics of the nonlinear model around the operating point of interest. To account for external disturbance and modeling inaccuracies, an output based robust multi-objective H_∞/H_2 control law integrated with pole placement has been proposed for the linearized model. The problem is solved by formulating linear matrix inequality (LMI) constraints for performance and robustness. The simulation results show that the designed controller gives adequate performance in the presence of modeling inaccuracies and external disturbance. Moreover, the results of the controller are compared with standard PI controller. The comparison shows that the performance of the designed technique is better in terms of tracking error and control energy utilization.

KEYWORDS
Energy conversion systems;Underground coal gasification (UCG) control; multi-objective H_∞/H_2 control;linear matrix inequalities (LMIs)

1. Introduction

Under ground coal gasification (UCG) in its most general form consists of two wells drilled from the surface to coal seam. In order to increase the permeability of coal, a link is established between the wells G. Perkins and Sahajwalla (2005). After the link establishment the oxidants (steam [H_2O (g)] and oxygen (O_2), O_2 or air) are injected from the injection well which chemically react with already ignited coal to produce synthesis or syngas (a mixture of carbon monoxide (CO), hydrogen (H_2), methane (CH_4) and some traces of higher hydro-carbons), which can be used in number of industrial applications G. Perkins and Sahajwalla (2005); Uppal, Bhatti, Aamir, Samar, and Khan (2014, 2015).

The control of UCG is an emerging area of research. In Kostur and Kacur (2011) a lab scale UCG setup is controlled by some versions of the conventional PID controller. The idea of UCG control system can not be mapped directly from lab scale set up to an actual field test, because it is not possible to create an actual UCG environment in lab experiments. One way to approach the problem of UCG control system design is to select an appropriate mathematical model, then a model based control strategy can be adopted for achieving the desired objective and finally, the idea can be implemented on the actual UCG site. In literature there are four different types of mathematical models of UCG, which differ mainly due to their chemical and physical assumptions, geometries, coal type and time and spacial domain characteristics G. M. P. Perkins (2005). These types include channel models F and S.M. (1975), packed bed models Winslow (1977), Khadse, Qayyumi, and Mahajani (2006); G. Perkins and Sahajwalla (2005); Thorsness and Rozsa (1978); Uppal et al. (2014), coal block models G. Perkins and Sahajwalla (2008) and process models Beizen (1996). Most of these models contain nonlinear partial differential equations (PDEs) with at least two independent variables, one each for time and space. The objective of these models is to carryout quantitative analysis of the UCG process.

The model based control of UCG has been investigated in Arshad, Bhatti, Samar, Ahmed, and Aamir (2012); Uppal, Alsmadi, Utkin, Bhatti, and Khan (2018); Uppal et al. (2015). In Arshad et al. (2012) a conventional sliding mode control (SMC) Fossard and Floquet (2002), based on equivalent control method has been developed for a simplified control oriented model of the UCG process to maintain a desired heating value of syngas. A similar control objective has been achieved by Uppal et al. (2018, 2015), however, Uppal et al. (2015) developed a super twisting SMC Levant (1993), whereas, a conventional SMC has been designed by Uppal et al. (2018). Moreover, in Uppal et al. (2018, 2015) partial differential equations based model of Uppal et al. (2014) is employed for the model based control.

The control of UCG based on infinite dimensional nonlinear process models Uppal et al. (2018, 2015) ensures global stability of the system, but at the expense of large computational resources and cost which are added due to complexities involve with the design Vasilyev (2008). Thus, it is better to have a linear model which retains the same input output behavior and easy for design and analysis Vasilyev (2008). In the literature few studies are available for linear model development pertaining to surface gasifiers Liu, Dixon, and Daley (2000); Wilson, Chew, and Jones (2006). However, there is no such work available for UCG.

In this research work a linear model of UCG has been developed, which is obtained by linearizing the model of Arshad et al. (2012). The results of linear model are compared with actual nonlinear model, which show a good match for the state variables and output of the system. The linear model is then used to develop the robust multi-objective control to maintain a desired heating value of the product gas. The controller integrates H_∞, H_2 and pole placement based methodologies to yield desired closed loop performance. The H_∞ control provides robustness against modeling inaccuracies and external disturbance, whereas, the H_2 control keeps the control effort within permissible range Doyle and Stein (1981); Skogestad and Postlethwaite (2007). Moreover, the pole placement technique improves the overall performance of the closed loop system. The multi-objective control problem is formulated in terms of linear matrix inequalities (LMIs), which provide a flexible way of describing coupled constraints Chilali and Gahinet (1996). Moreover, these LMIs are solved using Simulink and Natick (1993), which uses convex optimization framework and yields optimal global solution Boyd, El Ghaoui, Feron, and Balakrishnan (1994); Duan and Yu (2013); Scherer, Gahinet, and Chilali (1997). The proposed optimal and robust feedback compensation is then implemented on the actual nonlinear model. The simulation results show that the closed loop system meets the desired performance criteria.

The rest of the article is arranged as follows. In Section 2, the nonlinear time domain model of UCG is discussed. The problem statement and design procedure are formally presented in Sections 3 and 4, respectively. The linearization is discussed in Section 5, which is followed by the multi-objective control design in Section 6. The implementation of control scheme is given in Section 7, Section 8 presents the analysis of simulation results and the article is concluded in Section 9.

2. Nonlinear Model of UCG Process

This section presents nonlinear model of Arshad et al. (2012). The model is comprised of two solids: coal and char, and eight gases: CO, CO_2, H_2, CH_4, tar, H_2O, N_2 and O_2. The mathematical model given by (1) is comprised of mass and energy balances of the solids and gases.

$$
\begin{aligned}
\dot{\boldsymbol{x}}_1 &= -M_{coal}\boldsymbol{r}_1, \\
\dot{\boldsymbol{x}}_2 &= M_{char}\Big(0.766\boldsymbol{r}_1 - \boldsymbol{r}_2 - \boldsymbol{r}_3\Big), \\
\dot{\boldsymbol{x}}_3 &= \frac{1}{C_s}\Big(ht(Tg - \boldsymbol{x}_3) - \Delta H_2\boldsymbol{r}_2 - \Delta H_3\boldsymbol{r}_3\Big), \\
\dot{\boldsymbol{x}}_4 &= 0.008\boldsymbol{r}_1 + \boldsymbol{r}_3 - \beta\boldsymbol{x}_4, \\
\dot{\boldsymbol{x}}_5 &= 0.058\boldsymbol{r}_1 + \boldsymbol{r}_2 - \beta\boldsymbol{x}_5, \\
\dot{\boldsymbol{x}}_6 &= 0.083\boldsymbol{r}_1 + \boldsymbol{r}_3 - \beta\boldsymbol{x}_6, \\
\dot{\boldsymbol{x}}_7 &= 0.044\boldsymbol{r}_1 - \beta\boldsymbol{x}_7, \\
\dot{\boldsymbol{x}}_8 &= 0.0137\boldsymbol{r}_1 - \beta\boldsymbol{x}_8, \\
\dot{\boldsymbol{x}}_9 &= 0.055\boldsymbol{r}_1 + 0.075\boldsymbol{r}_2 - 0.925\boldsymbol{r}_3 + \frac{\alpha}{L}u - \beta\boldsymbol{x}_9 + \frac{1}{L}\delta, \\
\dot{\boldsymbol{x}}_{10} &= -1.02\boldsymbol{r}_2 + \frac{\lambda}{L}u - \beta\boldsymbol{x}_{10}, \\
\dot{\boldsymbol{x}}_{11} &= \frac{\zeta}{L}u - \beta\boldsymbol{x}_{11}.
\end{aligned}
\tag{1}
$$

Where $\boldsymbol{x}_1$, $\boldsymbol{x}_2$, $\boldsymbol{x}_3$ and $\boldsymbol{x}_i$, $i = 4, \ldots, 11$ represent densities of coal and char (g/cm^3), solid temperature (K) and concentration of gas i (mol/cm^3), respectively. The flow-rate of injected gases u (moles/cm^2/s) is the control input.

The output of the system is the calorific value or heating value of the product gases y (KJ/mol), which is given by

$$
\begin{aligned}
y &= mf_{CO}H_a + mf_{H_2}H_b + mf_{CH_4}H_c, \qquad (2)\\
mf_i &= \frac{C_i}{C_T}, \\
C_T &= \sum_{i=4}^{11} C_i.
\end{aligned}
$$

The remaining parameters of the nonlinear model are defined in Table 1, whereas, the chemical kinetics of the process is explained in A.

3. Problem Statement

The objective of this research work is to design a control system for UCG process, which maintains the heating value of product gas at a desired level. The designed control law should handle the modeling errors due to the linearization, and the effect of external disturbance δ.

4. Outline of Design Procedure

The design methodology is listed below:

(1) The nonlinear model of UCG is linearized around a particular operating point to develop a linear model.
(2) The design specifications of UCG process are formulated as LMIs and synthesized with robust design techniques.
(3) The designed feedback compensation is tested with actual nonlinear model to evaluate its performance.

5. Linear Model Development

The nonlinear model discussed in section 2 can be represented in the following form:

$$\begin{aligned} \dot{\boldsymbol{x}} &= \boldsymbol{f}(\boldsymbol{x}) + \boldsymbol{g}\boldsymbol{u}, \\ \boldsymbol{y} &= \boldsymbol{h}(\boldsymbol{x}). \end{aligned} \tag{3}$$

where $\boldsymbol{x}, \boldsymbol{f}, \boldsymbol{g}, \boldsymbol{h} \in \mathbb{R}^{11}$ and $\boldsymbol{u}, \boldsymbol{y} \in \mathbb{R}^{+}$ are scalars. The linearization is performed around a particular operating point (x^*, y^* and u^*) given in (4), which refers to the instance when the output reaches its maximum value. During the open loop simulations this operating point is reached at $t = 20000$ s (5.5 hrs).

$$\begin{aligned} \boldsymbol{x} &= [0.0001 \quad 0.3 \quad 850 \quad 0.0003 \quad 0.002 \quad 0.002 \\ &\qquad 0.001 \quad 0.003 \quad 0.001 \quad 0 \quad 0.001]^T \ , \\ \boldsymbol{y}^* &= 118 \ \text{ and } \boldsymbol{u}^* = 2 \times 10^{-04} \ . \end{aligned} \tag{4}$$

The state space of linear system is given by following equation:

$$\begin{aligned} \boldsymbol{\Delta}\dot{\boldsymbol{x}} &= \boldsymbol{A}\boldsymbol{\Delta}\boldsymbol{x} + \boldsymbol{B}\boldsymbol{\Delta}\boldsymbol{u} + d\boldsymbol{\delta}, \\ \boldsymbol{y} &= \boldsymbol{C}\boldsymbol{x} + \boldsymbol{D}u, \\ \boldsymbol{A} &= \left.\frac{\partial \boldsymbol{f}}{\partial \boldsymbol{x}}\right|_{x=x^*}, \\ \boldsymbol{B} &= \frac{1}{L}\begin{bmatrix} 0 & 0 & 0 & 0 & 0 & 0 \\ & 0 & 0 & \alpha & \lambda & \zeta \end{bmatrix}^T, \\ \boldsymbol{C} &= \left.\frac{\partial \boldsymbol{h}}{\partial \boldsymbol{x}}\right|_{\boldsymbol{x}=\boldsymbol{x}^*}, \\ \boldsymbol{D} &= 0. \end{aligned} \tag{5}$$

Where $\boldsymbol{A} \in \mathbb{R}^{11}$, $\boldsymbol{B} \in \mathbb{R}^{11\times 1}$, $\boldsymbol{C} \in \mathbb{R}^{1\times 11}$ and $\boldsymbol{D} \in \mathbb{R}^{+}$ are state space matrices.

In order to validate the model, the results are compared with the nonlinear model. The results presented in Figs. 1, 2, 3 and 4 show comparison of the coal and char densities, solid temperature and concentration and heating value of the product gases, respectively. It can be concluded from the open loop simulations that linear model adequately retains the dynamics of the nonlinear model in the vicinity of the operating point given in (4).

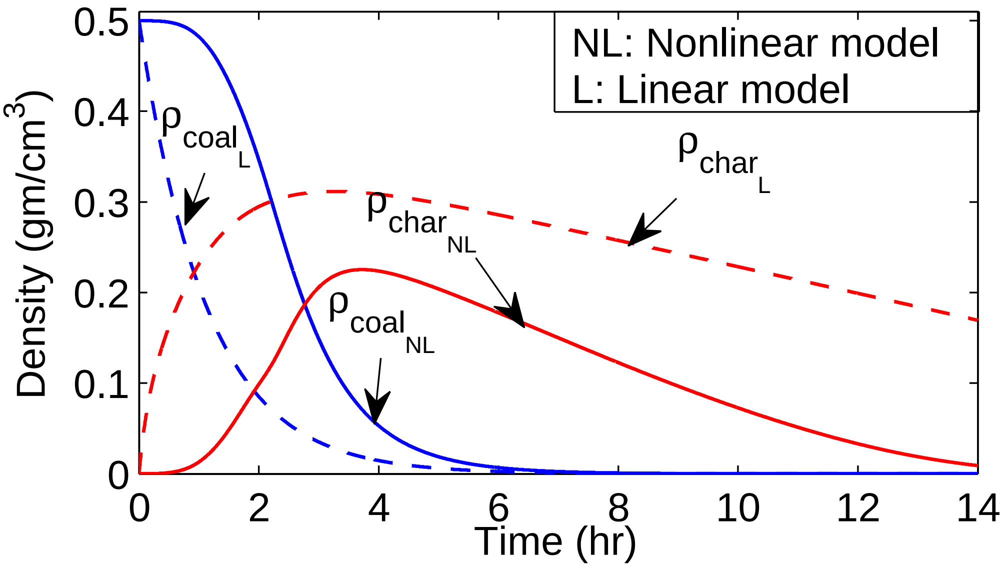

Figure 1. Linear and nonlinear densities of coal and char.

Initially, the linear system consists of eleven first order differential equations which have some uncontrollable and unobservable modes. Therefore, in order to make the system feasible for the subsequent controller synthesis, a minimal realization Brogan (1982) of the system is found. The resultant sixth order system given in (9) is both controllable and observable.

$$
\begin{aligned}
\boldsymbol{A} &= \begin{bmatrix}
-2.8\times10^{-3} & -1.77\times10^{-7} & -2\times10^{-15} & 9.62\times10^{-8} & -7.9\times10^{-8} & 9.63\times10^{-3}\\
1.22\times10^{-3} & -7.18\times10^{-6} & -2.2\times10^{-7} & -2.93\times10^{-6} & 1.6\times10^{-6} & -2.93\times10^{-6}\\
-3.3\times10^{-2} & -8.54\times10^{-6} & -2.8\times10^{-7} & 1.18\times10^{-4} & -6.4\times10^{-5} & 1.18\times10^{-4}\\
8.44 & 5\times10^{-7} & 1.6\times10^{-8} & -1\times10^{-4} & 1\times10^{-4} & -9.6\times10^{-5}\\
31.54 & 1\times10^{-9} & 3.3\times10^{-11} & 6.7\times10^{-5} & 1.4\times10^{-4} & 6.7\times10^{-5}\\
8.55 & -4.9\times10^{-7} & -1.6\times10^{-8} & -1\times10^{-4} & 1\times10^{-4} & -1.1\times10^{-4}
\end{bmatrix},\\
\boldsymbol{B} &= [-1.5\times10^{-3} \ -7.6\times10^{-3} \ -2.3\times10^{-4} \ 0 \ -1.298\times10^{-22} \ 0]^T,\\
\boldsymbol{C} &= [-2.5\times10^{-2} \ 5.1\times10^{-3} \ 1.7\times10^{-4} \ -3520 \ -19.51 \ 3559]. \qquad (6)
\end{aligned}
$$

6. Design of Multi-Objective H_2/H_∞ via Regional Pole Placement

The design specifications for the control design are discussed in the following sub-section.

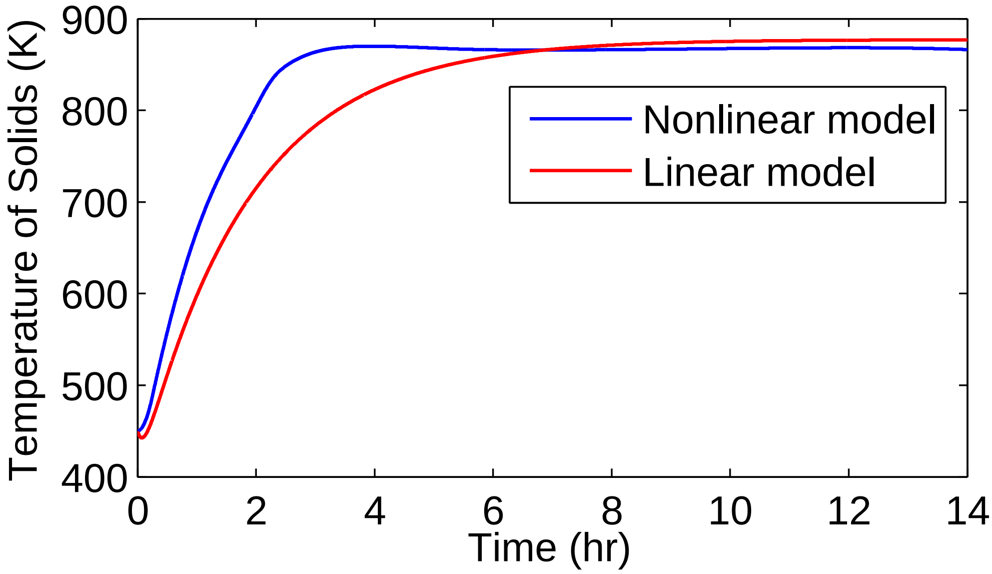

Figure 2. Comparison of linear and nonlinear solid temperatures.

6.1. Design Specifications

The bounded input disturbance d in (5) is modeled by the following second order transfer function

$$G_d(s) = \frac{2.27 \times 10^-13}{s^2 + 3.84 \times 10^{-04}s + 3.79 \times 10^{-08}}. \tag{7}$$

From (7), the bandwidth frequency of disturbance input is $\omega_d = 7 \times 10^{-04}(rad/sec)$. Therefore, in order to achieve disturbance rejection, the crossover frequency (ω_c) or closed loop bandwidth ω_b should be greater than ω_d Skogestad and Postlethwaite (2007). The other design specifications are bounded flow rate of injected gases $(0 < u_{min} \leq u \leq u_{max})$, and the allowable percentage overshoot is (PO$\leq$ 10%). These design specifications define the desired closed loop performance.

6.2. Multi-Objective Design

In order to satisfy all the design constraints, a multi-objective design methodology has been proposed. A general one degree of freedom design configuration given in Fig. 5 can be adopted to transform the multi-objective control problem in terms of LMIs. In this configuration $P(s)$ is the generalized linear time invariant system with inputs $w = \begin{bmatrix} r & d \end{bmatrix}^T$ and outputs $\begin{bmatrix} z_\infty & z_2 \end{bmatrix}^T$, where $z_\infty = y_r - y$ and $z_2 = u$. The state space realization of P(s) is given by

$$\begin{aligned} \dot{\boldsymbol{x}} &= \tilde{\boldsymbol{A}}\boldsymbol{x} + \boldsymbol{B}_1\boldsymbol{w} + \boldsymbol{B}_2\boldsymbol{u}, \\ \boldsymbol{z}_\infty &= \boldsymbol{C}_\infty\boldsymbol{x} + \boldsymbol{D}_{11}\boldsymbol{w} + \boldsymbol{D}_{12}\boldsymbol{u}, \\ \boldsymbol{z}_2 &= \boldsymbol{C}_2\boldsymbol{x} + \boldsymbol{D}_{21}\boldsymbol{w} + \boldsymbol{D}_{22}\boldsymbol{u}, \\ \boldsymbol{y} &= \boldsymbol{C}_y\boldsymbol{x} + \boldsymbol{D}_y\boldsymbol{u}. \end{aligned} \tag{8}$$

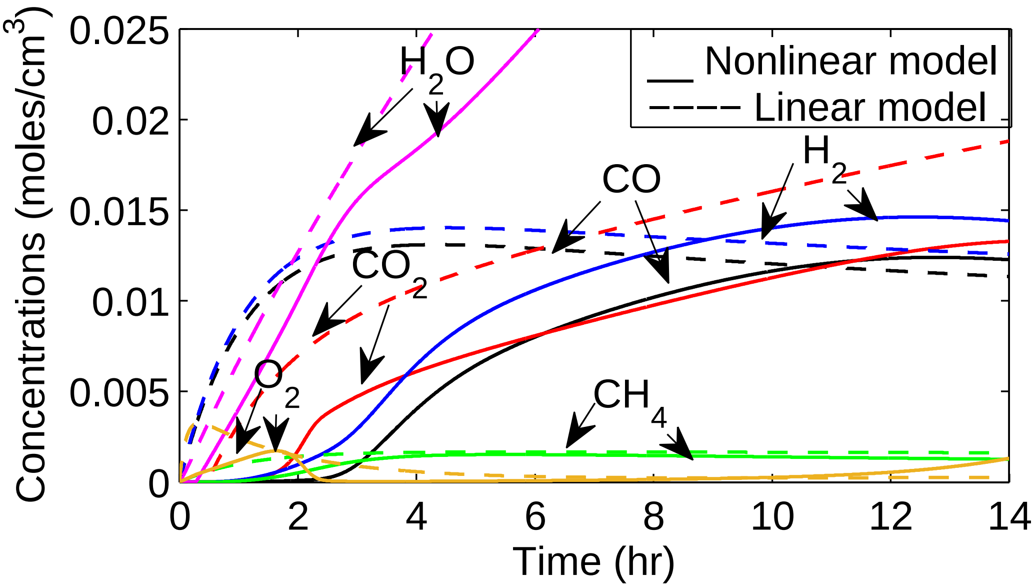

Figure 3. Concentration of product gases for linear and nonlinear models.

Where $\boldsymbol{x} \in \mathbb{R}^6$, $\boldsymbol{z} \in \mathbb{R}^2$ and $\boldsymbol{w}, \boldsymbol{u}, \boldsymbol{y} \in \mathbb{R}^+$. The state space matrices in (8) are given by

$$\tilde{\boldsymbol{A}} = \begin{bmatrix} -0.003 & -0.0010 & -0.0002 & -4.7\times10^{-5} & -1\times10^{-5} & -9.9\times10^{-7} \\ 0.00097 & 0 & 0 & 0 & 0 & 0 \\ 0 & 0.0004 & 0 & 0 & 0 & 0 \\ 0 & 0 & 6.1\times10^{-5} & 0 & 0 & 0 \\ 0 & 0 & 0 & 1.5\times10^{-5} & 0 & 0 \\ 0 & 0 & 0 & 0 & 9.5\times10^{-7} & 0 \end{bmatrix},$$

$$\tilde{\boldsymbol{B}} = \begin{bmatrix} 0 & 0 & 0 & 0 & 0 & 0 \\ 0 & 0 & 0 & 0 & 0 & 0 \\ 4 & 0 & 0 & 0 & 0 & 0 \end{bmatrix}^T, \quad \tilde{\boldsymbol{C}} = \begin{bmatrix} 0 & -0.006 & -0.04 & -0.28 & -1.26 & -0.03 \\ 0 & 0 & 0 & 0 & 0 & 0 \\ 0 & -0.0063 & -0.04 & -0.24 & -1.26 & -0.03 \end{bmatrix},$$

$$\tilde{\boldsymbol{D}} = \begin{bmatrix} \boldsymbol{D}_{11} & \boldsymbol{D}_{12} \\ \boldsymbol{0}^{1\times2} & \boldsymbol{D}_y \\ \boldsymbol{D}_{21} & \boldsymbol{D}_{22} \end{bmatrix} = \begin{bmatrix} 1 & -1 & 0 \\ 0 & 0 & 1 \\ 1 & -1 & 0 \end{bmatrix}. \tag{9}$$

Where $\tilde{\boldsymbol{B}} = \begin{bmatrix} \boldsymbol{B}_1 & \boldsymbol{B}_2 \end{bmatrix}$ and $\tilde{\boldsymbol{C}} = \begin{bmatrix} \boldsymbol{C}_\infty & \boldsymbol{C}_2 & \boldsymbol{C}_y \end{bmatrix}^T$.

The choice of exogenous input w and output z yields the following closed loop transfer functions: $T_{z_\infty,w} = S$ and $T_{z_2,w} = KS$ by employing feedback law $u = Ky$.

$$T_{z_\infty w}(s) = (C_\infty + D_{11}K)(sI - (A + B_1K)^{-1}B_2 + D_{12}, \tag{10}$$
$$T_{z_2 w}(s) = (C_2 + D_{21}K)(sI - (A + B_1K)^{-1}B_2. \tag{11}$$

Thus for robust stability, disturbance rejection and bounded control effort the peaks of closed loop transfer functions $\|T_{z_\infty w}(s)\|$ and $\|T_{z_2 w}(s)\|$ are minimized by some performance index γ as

$$\|T_{z_\infty w}(s)\| < \gamma_\infty, \quad \textit{and} \quad \|T_{z_2 w}(s)\| < \gamma_2. \tag{12}$$

Hence for UCG linear system given in (8), the output feedback law is designed, which ensures H_∞ and H_2 performances and regional closed loop pole placement $\lambda(A_{cl} \subset$

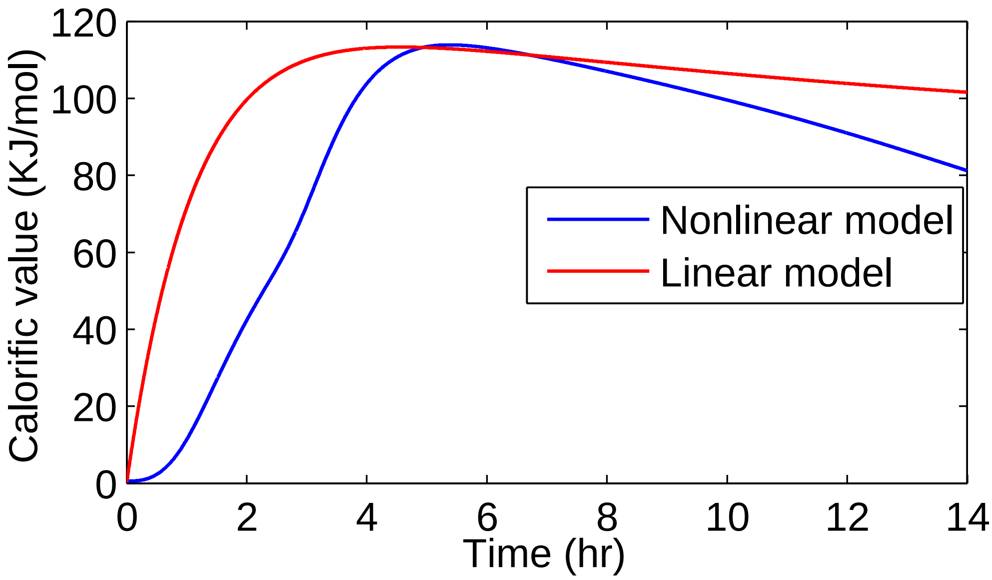

Figure 4. Comparison of caloric value of product gases for both linear and nonlinear models

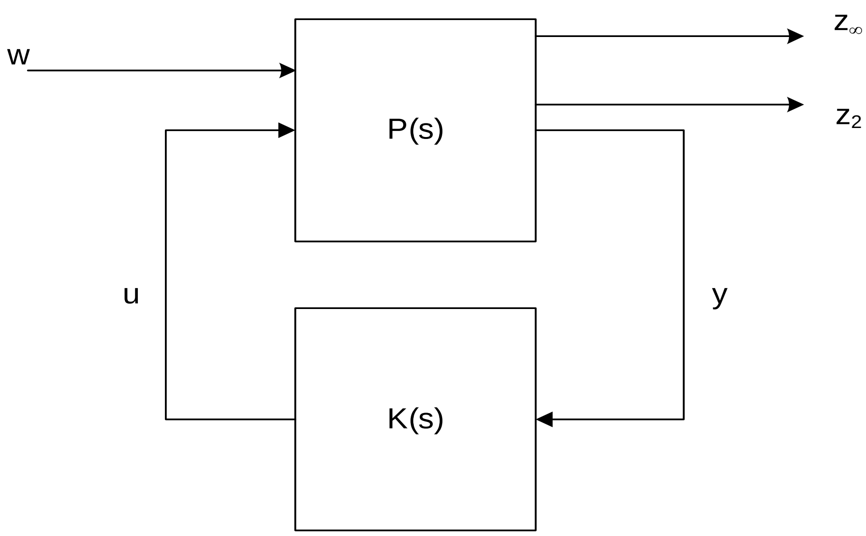

Figure 5. One degree of freedom control configuration Skogestad and Postlethwaite (2007)

D) requirement, by solving following LMI conditions:

6.2.1. H_∞ Performance Constraints

The H_∞ performance objective can be achieved if there exists a K such that $\|T_{z_\infty w}\| < \gamma_\infty$ holds, only if there exists a symmetric positive definite matrix P_∞ and a matrix

W_∞, such that following LMI conditions meet

$$\begin{bmatrix} (AP_\infty + B_1W_\infty)^T + AP_\infty + B_1W_\infty & B_2 & (C_\infty P_\infty + D_{\infty 1}W_\infty)^T \\ B_2^T & \gamma_\infty I & D_{\infty 2}^T \\ C_\infty P_\infty + D_{\infty 1}W_\infty & D_{\infty 2} & -\gamma_\infty I \end{bmatrix} < 0,$$
$$P_\infty > 0. \tag{13}$$

The feedback gain matrix can be calculated as $K = K_\infty = W_\infty P_\infty^{-1}$.

6.2.2. H_2 Performance Constraints

Similarly closed loop norm in terms of H_2 is satisfied if there exists a K such that $\|T_{z_2w}\| < \gamma_2$ holds, only if there exist two symmetric positive definite matrices P_2 and Z, and a matrix W_2, such that following LMI conditions meet

$$AP_2 + B_1W_2 + (AP_2 + B_1W_2)^T + B_2B_2^T < 0,$$
$$\begin{bmatrix} -Z & C_2P_2 + D_{21}W_2 \\ (C_2P_2 + D_{21}W_2)^T & P_2 \end{bmatrix} < 0,$$
$$Trace(Z) < \gamma^2. \tag{14}$$

and feedback gain matrix can be calculated as $K = K_2 = W_2P_2^{-1}$.

6.2.3. Pole Region Constraints

In order to obtain desired transient response, the closed loop poles of the system are placed in the prescribed region. Let D be a desired LMI region in open left half of the complex plane, which is also symmetric about the real axis

$$D = s|s \in C, L + sM + \bar{s}M^T < 0, \tag{15}$$

where L is a positive definite symmetric matrix ($L \in \mathbb{S}^m$) and $M \in \mathbb{R}^{m\times m}$.

For UCG system disk type LMI region (D) is selected by using following L and M matrices:

$$L = \begin{bmatrix} -r & q \\ q & -r \end{bmatrix} \quad and \quad M = \begin{bmatrix} 0 & 1 \\ 0 & 0 \end{bmatrix}, \tag{16}$$

where $r = -0.0025$ and $q = -0.0001$ represent the radius and position of the disk region, respectively. The region D also ensures that the closed response is sufficiently smooth, with damping ratio $\zeta >= 0.7$ and the minimum bandwidth requirement $\omega_b \geq \omega_d$ is also satisfied. The closed loop poles will be in D, if there exists a matrix W_D and positive definite symmetric matrix P_D such that following LMI condition exists

$$L \otimes P_D + M \otimes (AP_D + B_1W_D) + M^T \otimes (AP_D + B_1W_D)^T < 0, \tag{17}$$

where $\otimes$ represents the Kronecker product.

Thus by specifying (D), parameterized by L and M matrices, the values of W_D and P_D can be computed by solving (17) which can be re-written as

$$\begin{bmatrix} -rP_D & qP_D + Q \\ qP_D + Q^T & -rP_D \end{bmatrix} < 0, \tag{18}$$

where $Q = AP_D + B_1W$ and feedback gain matrix $K = K_D = W_D P_D^{-1}$. The solution exists only if all LMIs related to respective constraints given by (13), (14) and (18) have feasibility in a common intersection region. This LMI optimization problem is solved by using Gahinet, Nemirovskii, Laub, and Chilali (1994), which yields a common compensator K as given in (19).

$$K = W_\infty P_\infty^{-1} = W_2 P_2^{-1} = W_D P_D^{-1}. \tag{19}$$

The implementation of the designed controller on the UCG system is discussed in the following section.

7. Implementation of Control Scheme

The configuration for UCG control system has been shown in Fig. 6. In order to assess the robustness of the multi-objective control design against unmodeled dynamics and external disturbance, the controller is implemented on the actual nonlinear model of Arshad et al. (2012). Moreover, the dynamics of the control valve and the gas analyzer have also been considered, which are given by following transfer functions Uppal et al. (2018):

$$G_1(s) = \frac{\exp(-\tau_{d_a} s)}{\tau_a s + 1} \approx \frac{-\tau_{d_a} s + 2}{\tau_a \tau_{d_a} s^2 + (2\tau_a + \tau_{d_a})s + 2}, \tag{20}$$

$$G_2(s) = \frac{\exp(-\tau_{d_g} s)}{\tau_g s + 1} \approx \frac{-\tau_{d_g} s + 2}{\tau_g \tau_{d_g} s^2 + (2\tau_g + \tau_{d_g})s + 2}, \tag{21}$$

where $\tau_a, \tau_g = 10\ s$ are the time constants for control valve and the gas analyzer respectively and $\tau_{d_a}, \tau_{d_g} = 10\ s$ represent the input and output time delays. The time delays in both control valve and the gas analyzer are replaced with first order Pade approximation.

Here it is pertinent to mention that total transport delay is $\theta_d = 20$s. The sufficient condition for closed loop stability in the presence of time delays is Skogestad and Postlethwaite (2007)

$$\omega_c \leq \frac{1}{\theta_d}, \tag{22}$$

where ω_c is the cross-over frequency for the magnitude plot of the loop gain transfer function $L = GK$. It can be seen from Fig. 7 that the condition in (22) is satisfied as $\omega_c = 9 \times 10^{-04} < 0.05$ rads/sec.

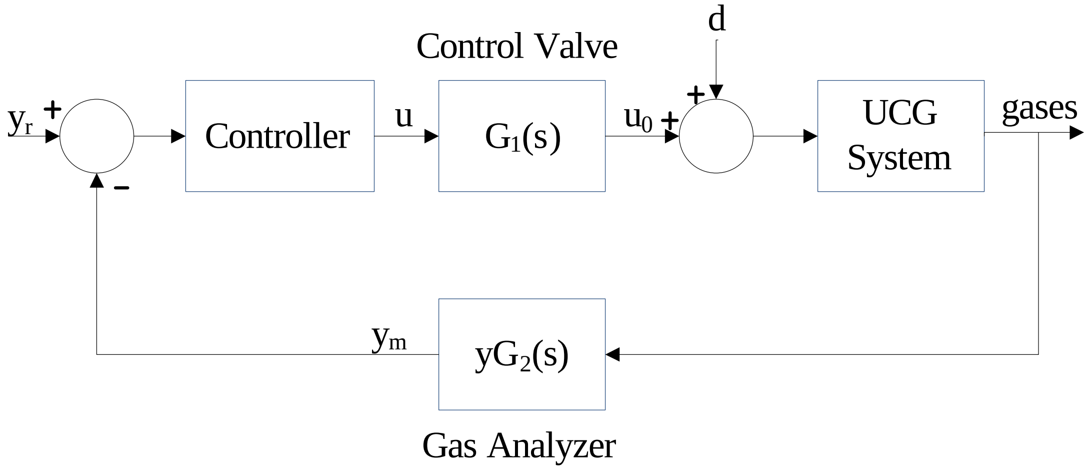

Figure 6. Block diagram of UCG control system Uppal et al. (2018).

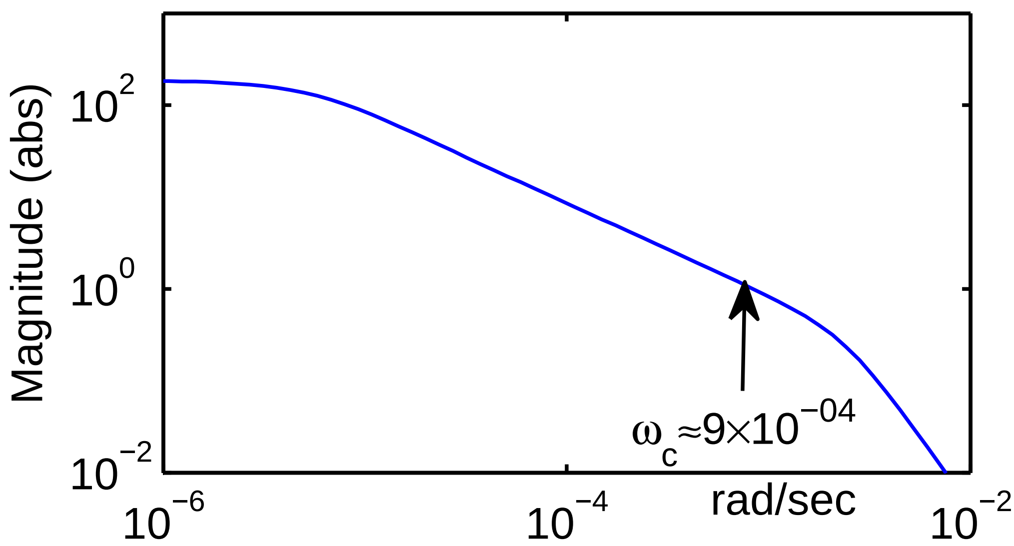

Figure 7. Magnitude Response of L=GK

8. Results and Discussions

The simulation results for the closed loop system shown in Fig. 6, employing the multi-objective controller (MOC), given by (19) are discussed in this section. In order to assess the performance of the proposed controller, a comparison has been made with conventional PI controller.

Prior to gasification, the coal seam is ignited in order to make the temperature of the UCG reactor feasible for the subsequent oxidation and gasification reactions. Therefore, the system operates in the ignition phase for first 1000 s. During the gasification phase, system is operated in open loop with flow-rate $u = 2 \times 10^{-4}$ moles/cm^2/s for 20000 s (5.5 hr), before the controller is brought in the loop.

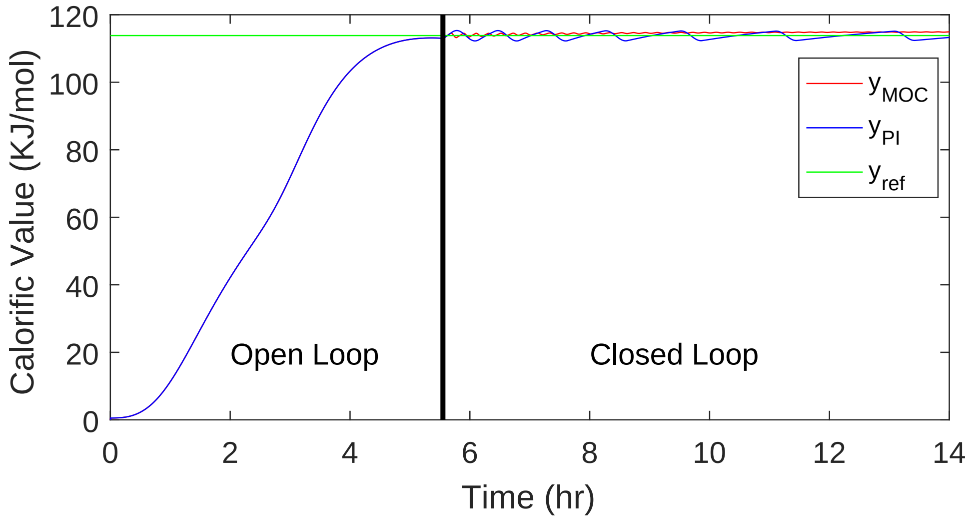

Figure 8. Calorific value of the system for PI and MOC

As shown in Fig. 8, the control effort in Fig. 9 successfully keeps the output at the desired level. The tacking error is also shown in Fig. 10. The process of UCG is very sensitive to the amount of H_2O residing in the reactor. As it favors the steam gasification reaction and hence the production of CO and H2. However, if excess water enters the reactor it can reduce the temperature feasible for the gasification reactions. It can be seen from Fig. 11 that the flow rate of H_2O produced from water entering from the surrounding aquifers acts as a disturbance for UCG control system. The controller caters for the disturbance by manipulating the flow rate of the injected gases (Fig. 9). When the water intrusion increases, the controller decreases the amount of H_2O entering in the reactor by reducing the flow rate of injected gases, hence maintaining an optimum amount of H_2O in the reactor. Apart from H_2O, the controller also maintains an optimum amount of O_2 in the reactor. Therefore, the controller sets the amounts of injected gases in such a way that the desired heating value is achieved in the presence of water intrusion and modeling inaccuracies.

The RMS values of the tracking error (e_{rms}) and the average power of the control signal (p_{avg}) for MOC and PI controllers is also compared. The expression for e_{rms} is given as

$$\mathrm{e}_{rms} = \sqrt{\frac{1}{N}\sum_{i=1}^{N} e(i)^2}\ , e(i) = y(i) - y_{ref}(i), \tag{23}$$

where N is the number of data points.

Whereas, p_{avg} has the following expression

$$\mathrm{p}_{avg} = \frac{1}{N}\sum_{i=1}^{N} u(i)^2\ . \tag{24}$$

The results in Table. 2, show the quantitative comparison of both the controllers. It is obvious that MOC consumes lesser control energy and yields smaller e_{rms} as

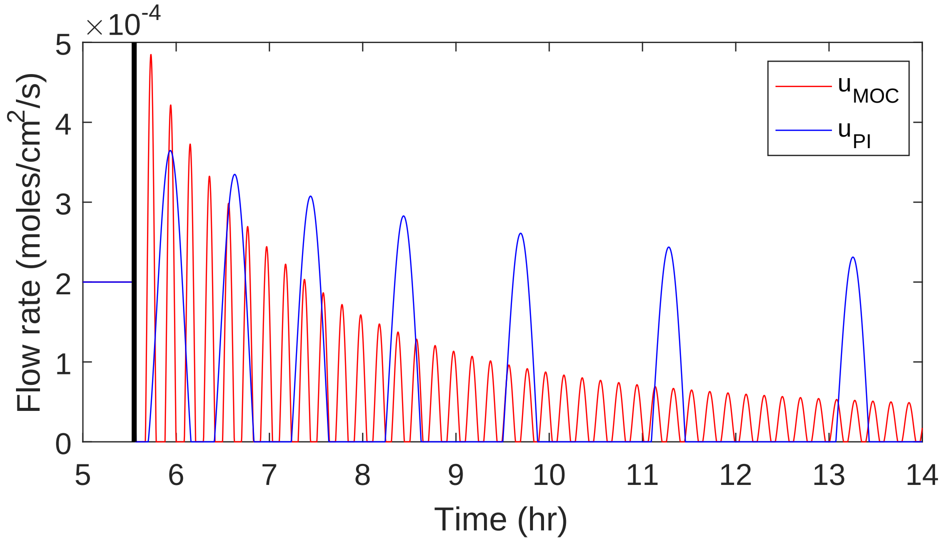

Figure 9. Flow-rate of the injected gases

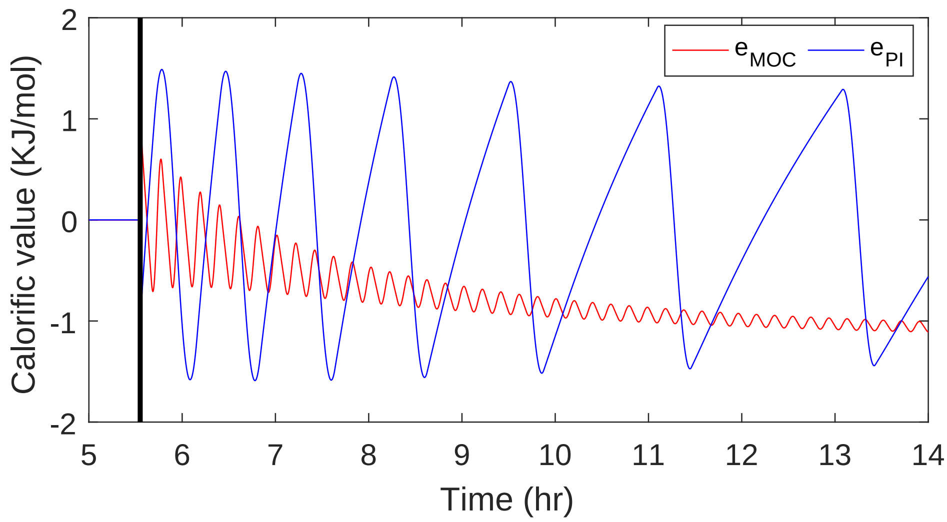

Figure 10. Error comparison for PI and MOC

compared to PI controller

9. Conclusion

In this work a linear model of UCG has been developed. The developed model is simple and requires less computational resources as compared to the original nonlinear model. Furthermore, the design specifications of UCG process are formulated as LMIs and synthesized as robust multi-objective H_2/H_∞ with regional pole placement problem. The developed robust compensator has been implemented on actual nonlinear model of UCG. Moreover, the dynamics of control valve, gas analyzer and water influx are also considered during the implementation to evaluate the robustness of the controller

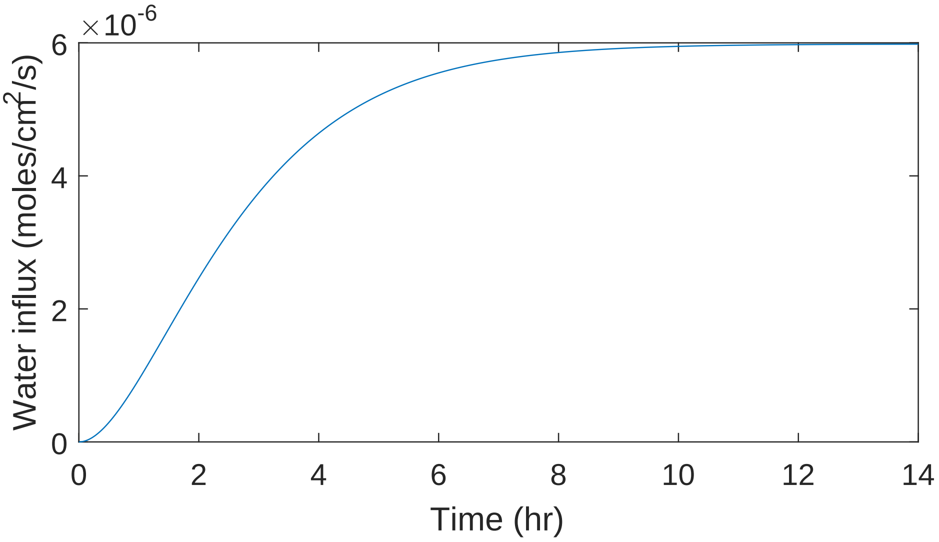

Figure 11. Flow-rate of the water influx

against modeling inaccuracies and external disturbance. The simulation results show that controller exhibits good performance despite all the imperfections. The quantitative comparison of the designed controller with PI controller shows that the former utilizes lesser control energy and yields smaller tracking error.

Appendix A. Chemical Kinetics

A large number of chemical reactions take place in a UCG reactor, however for convenience only three chemical reactions are considered in this work, which are given in Table A1. The mathematical expressions for the reaction rates of the selected reactions are given by

$$r_1 = 5\frac{x_1}{M_{coal}} \exp\left(\frac{-6039}{x_4}\right). \tag{A1}$$

$$r_2 = \frac{1}{\frac{1}{r_{c_2}} + \frac{1}{r_{m_2}}}, \tag{A2}$$

$$r_{c_2} = \frac{9.55 \times 10^8 x_2 m_{O_2} P \exp\left(\frac{-22142}{x_4}\right) x_4^{-0.5}}{M_{char}},$$

$$r_{m_2} = k_y m_{O_2} \quad and \quad k_y = 0.1 h_t,$$

$$r_3 = \frac{1}{\frac{1}{r_{c_3}} + \frac{1}{k_y m_{H_2O}}}, \tag{A3}$$

$$r_{c_3} = A\frac{r_{cc_3}}{m_{H_2O}} \quad and \quad A = m_{H_2O} - \frac{m_{H_2} m_{CO}}{k_{e_3}},$$

$$r_{cc_3} = \frac{\rho_{char} m_{H_2O}^2 P^2 \exp\left(5.052 - \frac{12908}{T_s}\right)}{M_{char}\left[m_6 P + \exp\left(-22.216 \frac{24880}{T_s}\right)\right]^2}.$$

Where k_{e_3} the equilibrium constant for steam gasification reaction, P the gas pressure (atm), and $k_y$the mass transfer coefficient and m_i represents the molar fraction of gas i.

$CH_{0.912}O_{0.194}$, $CH_{0.15}O_{0.02}$ and $(CH_{2.782})_9$ in Table. A1 are molecular formulas of coal, char and tar respectively.

References

Arshad, A., Bhatti, A. I., Samar, R., Ahmed, Q., & Aamir, E. (2012). Model development of ucg and calorific value maintenance via sliding mode control. In *Emerging technologies (icet), 2012 international conference on* (pp. 1–6).

Beizen, E. N. J. (1996). *Modeling underground coal gasification* (Unpublished doctoral dissertation). Delft University of Technology, Delft, Neitherlands.

Boyd, S., El Ghaoui, L., Feron, E., & Balakrishnan, V. (1994). *Linear matrix inequalities in system and control theory.* SIAM.

Brogan, W. L. (1982). *Modern control theory.* Pearson education india.

Chilali, M., & Gahinet, P. (1996). H/sub/spl infin//design with pole placement constraints: an lmi approach. *IEEE Transactions on automatic control*, *41*(3), 358–367.

Doyle, J., & Stein, G. (1981). Multivariable feedback design: Concepts for a classical/modern synthesis. *IEEE transactions on Automatic Control*, *26*(1), 4–16.

Duan, G.-R., & Yu, H.-H. (2013). *Lmis in control systems: analysis, design and applications.* CRC press.

F, M. C., & S.M., F. A. (1975). *A two-dimensional mathematical model of the underground coal gasification process.* Fall Meeting of the Society of Petroleum Engineers of AIME, 28 September-1 October 1975, Dallas, Texas.

Fossard, A., & Floquet, T. (2002). An overview of classical sliding mode control. In J. P. Barbot & W. Perruquetti (Eds.), *Sliding mode control in engineering.* New York, NY, USA: Marcel Dekker, Inc.

Gahinet, P., Nemirovskii, A., Laub, A. J., & Chilali, M. (1994). The lmi control toolbox. In *Decision and control, 1994., proceedings of the 33rd ieee conference on* (Vol. 3, pp. 2038–

2041).
Khadse, A., Qayyumi, M., & Mahajani, S. (2006). Reactor model for the underground coal gasification (ucg) channel. *International Journal of Chemical Reactor Engineering*, *4*, – ST - Reactor model for the underground coal gas.
Kostur, K., & Kacur, J. (2011, may). Development of control and monitoring system of ucg by promotic. In *Carpathian control conference (iccc), 2011 12th international* (p. 215 -219).
Levant, A. (1993). Sliding order and sliding accuracy in sliding mode control. *International journal of control*, *58*(6), 1247–1263.
Liu, G., Dixon, R., & Daley, S. (2000). Multi-objective optimal-tuning proportional-integral controller design for the alstom gasifier problem. *Proceedings of the Institution of Mechanical Engineers, Part I: Journal of Systems and Control Engineering*, *214*(6), 395–404.
Perkins, G., & Sahajwalla, V. (2005). A mathematical model for the chemical reaction of a semi-infinite block of coal in underground coal gasification. *Energy & Fuels*, *19*(4), 1679–1692. Retrieved from http://pubs.acs.org/doi/abs/10.1021/ef0496808
Perkins, G., & Sahajwalla, V. (2008). Steady-state model for estimating gas production from underground coal gasification. *Energy & Fuels*, *22*(6), 3902–3914. Retrieved from http://pubs.acs.org/doi/abs/10.1021/ef8001444
Perkins, G. M. P. (2005). *Mathematical modelling of underground coal gasification* (Unpublished doctoral dissertation). The University of New South Wales.
Scherer, C., Gahinet, P., & Chilali, M. (1997). Multiobjective output-feedback control via lmi optimization. *IEEE Transactions on automatic control*, *42*(7), 896–911.
Simulink, M., & Natick, M. (1993). *The mathworks.* Inc.
Skogestad, S., & Postlethwaite, I. (2007). *Multivariable feedback control: analysis and design* (Vol. 2). Wiley New York.
Thorsness, C. B., & Rozsa, R. B. (1978). Insitu coal-gasification - model calculations and laboratory experiments. *Society of Petroleum Engineers Journal*, *18*, 105–116 ST - Insitu Coal-Gasification - Model Cal.
Uppal, A. A., Alsmadi, Y. M., Utkin, V. I., Bhatti, A. I., & Khan, S. A. (2018, March). Sliding mode control of underground coal gasification energy conversion process. *IEEE Transactions on Control Systems Technology*, *26*(2), 587-598.
Uppal, A. A., Bhatti, A. I., Aamir, E., Samar, R., & Khan, S. A. (2014). Control oriented modeling and optimization of one dimensional packed bed model of underground coal gasification. *Journal of Process Control*, *24*(1), 269 - 277.
Uppal, A. A., Bhatti, A. I., Aamir, E., Samar, R., & Khan, S. A. (2015). Optimization and control of one dimensional packed bed model of underground coal gasification. *Journal of Process Control*, *35*, 11 - 20.
Vasilyev, D. M. (2008). *Theoretical and practical aspects of linear and nonlinear model order reduction techniques* (Unpublished doctoral dissertation). Massachusetts Institute of Technology.
Wilson, J., Chew, M., & Jones, W. (2006). State estimation-based control of a coal gasifier. *IEE Proceedings-Control Theory and Applications*, *153*(3), 268–276.
Winslow, A. M. (1977). Numerical model of coal gasification in a packed bed. In *16th symposium on combustion (international)* (p. 503-513).

Table 1. List of Parameters.

Symbol	Description	Units
M_{coal}, M_{char}	Molecular weight of coal and char	g/mol
T_g	Gas temperature	K
ΔH_j	Heat of the j_{th} chemical reaction	cal/mol
h_t	Heat transfer coefficient	cal/s/K/cm^3
L	Length of reactor	cm
C_s	Heat capacity of solids	cal/g/K
β	Model parameter Arshad et al. (2012)	$1/s$
δ	Flow rate of water influx (matched disturbance)	moles/cm^2/s
α, λ and ζ	Model parameters defining the weightage of H_2O, O_2 and N_2 in u	$--$

Table 2. Performance comparison for MOC and PI controllers.

Controller	e_{rms}	p_{avg}
PI	0.9295	1.3696×10^{-8}
MOC	0.8196	8.8478×10^{-9}

Table A1. List of Chemical Reactions considered in model.

Sr.	chemical equations
1.	Pyrolysis $CH_{0.912}O_{0.194} \overset{r_1}{\to} 0.766CH_{0.15}O_{0.02} +0.008CO+0.055H_2O+0.083H_2+0.044CH_4 +0.058CO_2+\frac{0.124}{9}(CH_{2.782})_9$
2.	Char Oxidation $CH_{0.15}O_{0.02}+1.028O_2 \overset{r_2}{\to} CO_2+0.075H_2O$
3.	Steam gasification $CH_{0.15}O_{0.02}+0.955H_2O \overset{r_3}{\leftrightarrow} CO+H_2$